

2. V. I. Fisher, "Fast wave of gas ionization in a power laser beam," Zh. Éksp. Teor. Fiz., 79, No. 6 (1980).
3. V. I. Fisher, "Supersonic regimes of propagation of an ionization wave along a laser beam," Zh. Tekh. Fiz., 53, No. 11 (1983).
4. I. Z. Nemtsev and B. F. Mul'chenko, "Laser-maintained fast ionization wave in xenon," Fiz. Plazmy, 3, No. 5 (1977).
5. I. É. Markovich, I. V. Nemchinov et al., "Superdetonation waves in air propagating toward a laser beam," Pis'ma Zh. Tekh. Fiz., 3, No. 3 (1977).
6. V. A. Boiko, V. V. Vladimirov et al., "Supersonic radiation waves in gases under the action of CO₂ laser radiation," Pis'ma Zh. Tekh. Fiz., 4, No. 22 (1978).
7. V. A. Boiko, V. A. Danilychev et al., "Observation of supersonic radiation waves in gases under the action of CO₂ laser radiation," Kvant. Élektron., 5, No. 1 (1978).
8. V. I. Fisher and V. M. Kharash, "Superdetonation motion of a plasma front toward a powerful laser beam," Zh. Éksp. Teor. Fiz., 82, No. 3 (1982).
9. V. I. Fisher, "Change of regime with supersonic propagation of a discharge," Pis'ma Zh. Tekh. Fiz., 10, No. 21 (1984).
10. M. F. Ivanov, "Propagation of optical breakdown waves in gases," Kvantovaya Élektron., 5, No. 12 (1978).
11. V. A. Gal'burt and M. F. Ivanov, "Nonstationary optical breakdown wave in hydrogen," Zh. Tekh. Fiz., 49, No. 12 (1978).
12. F. V. Bunkin and V. V. Savranskii, "Optical breakdown of gases initiated by a thermal explosion of suspended macroscopic particles," Zh. Éksp. Teor. Fiz., 65, No. 6 (1973).
13. S. I. Anisimov and V. I. Fisher, "Ionization relaxation and absorption of light behind a strong shock wave in hydrogen," Zh. Tekh. Fiz., 41, No. 12 (1971).
14. Ya. B. Zel'dovich and Yu. P. Raizer, Physics of Shock Waves and High-Temperature Hydrodynamic Phenomena [in Russian], Nauka, Moscow (1966).
15. N. N. Magretova, N. T. Pashchenko, and Yu. P. Raizer, "Structure of a shock wave with multiple ionization of atoms," Zh. Prikl. Mekh. Tekh. Fiz., No. 5 (1970).

FEATURES OF IONIZATION AND EMISSION BEHIND STRONG SHOCK WAVES IN AIR

V. A. Gorelov and L. A. Kil'dyushova

UDC 533.6.001.72

In 1960-1970 numerous experiments were carried out for studying emission processes in air (see, e.g., [1]) on the basis of shock tubes. Studies embraced a wide spectral range ($\lambda = 200-6000$ nm), and equilibrium values of temperature 2000-14,000 K with gas pressure $p_0 > 13$ Pa. On the basis of experiments the role of different emission processes was established and values of parameters required for quantum mechanics calculations for emission were specified. Results of detailed calculations of emission equilibrium for air are presented in tables in [1, 2].

By comparing calculated values for spectral intensity of emission for air from these experimental works it is possible to draw the following conclusions. The main mass of experimental results obtained in shock tubes relate to values $T \leq 10^4$ K and $\rho \geq 10^{-3} \rho_0$ (ρ_0 is density under normal conditions, ρ is gas density). There is good conformity between results of experiments and calculations. A more complex situation is observed in analyzing data found at higher temperatures and low values of ρ . A considerable proportion of experiments with $T > 10^4$ K were carried out in shock tubes with observation of emission in the region behind the reflected shock wave (SW) with relatively high gas density and pressure. With low pressures and $T > 10^4$ K the study of emission capacity was carried in a few works (e.g., [3, 4]). In them experimental conditions were not analyzed for explaining the presence behind the shock wave of local thermodynamic equilibrium (LTE). It was assumed that in the region behind the SW, corresponding to the output of the recorded signal of the emission receiver at a quasi-steady level, LTE exists. Values of spectral emission intensity obtained under these conditions ($\lambda = 500, 6100$ nm) with $v_s > 11$ km/sec are markedly below the corresponding calculated values (if the calculation is carried out using [1, 2]).

In [5] attention is drawn to the fact that under shock tube conditions operating in a high velocity mode ($v_s > 9$ km/sec) and low initial air pressures ($p_0 < 132$ Pa), when the main ionizing process becomes electron shock in a quasisteady sample of heated gas, behind the SW there may not be observation of LTE as a result of lighting up of emission in lines and depletion of the population density of excited atom levels. Absence of LTE develops in a reduced value of electron concentration n_e in the gas sample behind the SW [5, 6]. The effect of a reduction in n_e compared with the equilibrium level with $v_s > 9$ km/sec and $p_0 = 13$ Pa was apparently first observed in [7]. Reduction in the degree of ionization in the case of disturbing the LTE condition should in a marked way affect gas parameters in the gas sample since with $v_s > 9$ km/sec ionization of air behind the SW becomes a power-consuming process. Under these conditions it is possible to expect marked deviation of gas emission characteristics in the shock layer from equilibrium values. In [5] it was found that with $v_s = 12$ km/sec and $p_0 = 26$ Pa emission in the oxygen line ($\lambda = 773.3$ nm) is less by more than a factor of forty than the corresponding equilibrium value. However, there are no data for systematic study of the emission characteristics of air under the conditions given above, and this served as a basis for the present work where, apart from the results of measuring the emission characteristics, results are given from experiments for measuring ion concentration, electron temperature, and the excitation temperature for oxygen atoms.

1. Experiments for studying gas parameters behind a strong SW were carried out in an electrical discharge shock tube [8], and in them a study was made of SW propagating in a channel with length $l = 4-5$ m with different internal diameter ($d = 35, 57, 110$ mm). The main part of the channel was a glass tube (wall thickness 5-10 mm) which ended in a steel chamber with a viewing port and an ionization sensor for determining incident SW velocity v_s . The accuracy of determining v_s by a system with a digital counter was $\sim 2\%$. The whole channel of the tube was cleaned after three starts, and before each start the glass in the viewing port was changed. Before the start the channel was evacuated and filled with pure air to $p_0 = 66-6.6$ Pa. The main part of the experiments was carried with $p_0 = 26$ Pa. In control starts air was continuously pumped with the prescribed pressure.

In spectral studies use was made of a four-channel diffraction spectrometer DFS-33. With $\lambda < 600$ nm measurements were carried out in the second order spectrum (linear dispersion ~ 1.3 nm/mm) using an FEU-18 photomultiplier, and with $\lambda > 600$ nm they were carried out in a first order spectrum with an FEU-22. Signals from the photomultiplier through a preliminary amplifier entered an S8-2 oscillograph. Units with photomultipliers in the prescribed section of the spectrum were monitored for spectra of Hg, He, H₂ with $\lambda \leq 600$ nm, and for neon lines in the infrared region. The error in setting up the inlet slit of the photomultiplier unit in the continuous spectrum region for air did not exceed ± 1 nm. Tuning accuracy for test lines O1 in the infrared region was carried out from the spectrum for air from a spark discharge between copper electrodes. Discharge was initiated by a spark generator IG-3.

In order to reduce systematic errors in measuring emission intensity use was made of two types of optical illumination systems for the inlet slit. The two-lens system exhibited considerable luminosity, and the single-lens system guaranteed absence of vignetting. Glass light filters were used in order to separate series with simultaneous recording in the visible and infrared regions of the spectrum.

Energy calibration for the recording channels was carried out by a tungsten lamp SI-6-100, and metrological calibration of the lamp was carried out in a constant current supply mode from a stabilized source MTKS-35 at a wavelength $\lambda = 650$ nm. Calibration data for the spectrum was converted on the basis of results in [9].

Concentration of ions in the sample behind the SW was determined by means of expendable cylindrical electrostatic probes with a probe radius $r_p = 80$ μm (Knudsen number $Kn \approx 1$ with $p_0 = 26$ Pa), and probe voltage $V = -10$ V. Prior studies for probe functioning under experimental conditions were carried out as in [10]. With $v_s > 9$ km/sec probe measurements were monitored by measuring n_e according to the Stark broadening of the H β line [6].

Electron temperature T_e was determined by means of a variant of the "floating" triple probe [11]. Three cylindrical probe electrodes $P_1, P_2,$ and P_3 with diameter 80 μm and length of the working section 2 mm were placed at distance of 2.5 mm from each other. Apart from cylindrical electrodes in some of the experiments use was made of flat electrodes 2 \times 7 mm in size (thickness ~ 0.1 mm). All of the probes were of one-time use, and before the start they were cleaned with a glow discharge. A voltage of ~ 5 V was supplied to electrodes P_2-P_3 from an insulated source, and the difference in potential $V_{1,2}$ between electrodes $P_1 - P_2$

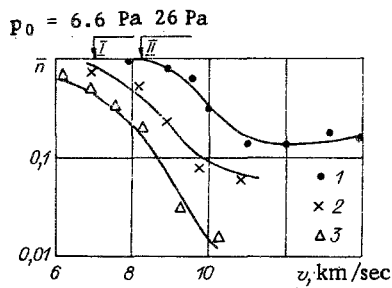


Fig. 1

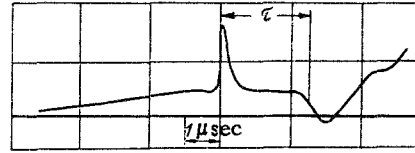


Fig. 2

was recorded by a differential system with a high input. In a simplified variant [11] the relationship between $V_{1,2}$ and T_e has the form $V_{1,2} = (kT_e/2) \ln 2$. Analysis of the results given below for determining T_e by this method showed that with $v_s = 6.5-9.5$ km/sec the measured quasisteady values of T_e in the gas sample behind the SW agree with the corresponding calculated equilibrium values.

2. Results of measuring n_e behind the SW with $p_0 = 6.6-26$ Pa are given in Fig. 1. Along the axis is set the ratio of measured values of n_e to the corresponding equilibrium values [12]: $\bar{n} = n_e/n_{ep}$ (points 1-3 relate to $p_0 = 26; 13; 6.6$ Pa and $d = 57; 102; 102$ mm). Arrows I and II around the abscissa axis show values of $v_{sI,II}$ with which in the equilibrium calculation [12] concentrations of NO^+ and N^+ are compared. With $v_s > v_{sI,II}$ the main ionization mechanism becomes electron shock. A marked difference can be seen in measured values of n_e in the sample behind the SW from the corresponding n_{ep} .

Given in Fig. 2 is the type of signal oscillogram with a triple probe during recording of T_e ($p_0 = 13$ Pa, $v_s = 9.7$ km/sec). The value of the signal is proportional to T_e . Its characteristic features are noted. Ahead of the SW front a smooth increase in T_e is observed in the zone of preceding ionization. Directly behind the front in all of the test v_s range there is a clear signal peak which points to the presence of a zone of high value of T_e in the relaxation region of the shock front. With $v_s > 8$ km/sec after the initial peak T_e emerges into a quasisteady level within the shock-heated gas sample. With $v_s \leq 7.5$ km/sec after the peak the T_e signal falls to a certain minimum value followed by an increase in it to the corresponding quasisteady level.

Presented in Fig. 3 are $T_e = f(v_s)$ dependences for the quasisteady region (points 1 and 2) and the maximum T_e in the nonequilibrium peak (points 3 and 4). Maximum values of T_e in the peak may be low as a result of insufficient spatial rarefaction ($\Delta x = 2$ mm). Line I is calculation of T behind the SW for an ideal gas, III is the calculated equilibrium temperature T_p behind the SW. It can be seen that with $v_s \leq 9$ km/sec measured values of T_{es} in the quasisteady region agree with T_p . With high velocities $T_{es} > T_p$ and with $v_s = 12$ km/sec, $T_{es}/T_p \approx 2-2.5$.

Results of measuring the spectral emission coefficient j_λ at wavelengths $\lambda = 510$ and 520 nm are given in Fig. 4 (point 1). Since in experiments with fixed values of v_s there was no marked difference in values of j_λ with $\lambda = 510$ and 520 nm, in Fig. 4 they are labeled identically. Curve I is calculation of j_λ with $\lambda = 510$ nm under equilibrium conditions from tables in [1, 2]. It can be seen that with $v_s \leq 9$ km/sec experimental values of j_λ agree with calculated values, but with high SW velocities measured values of j_λ are markedly (by a factor of four-six with $v_s = 10-12$ km/sec) less than calculated values.

An approximate calculation was made of the relationship $j_\lambda = f(v_s)$ with $\lambda = 510$ nm taking account of the results of experiments for measuring n_e with $v_s = 8-12$ km/sec. It was assumed that all of the molecular absorption coefficients [in systems $N_2(1+)$, $N_2^+(1-)$, $NO(\beta)$] relate to equilibrium values of p and T behind the SW according to [1, 2]. In calculations of absorption coefficients in free-free and free-bounded transitions use was made of equilibrium values for N , O , and NO and n_e and n_i measured by experiment. The absorption coefficient caused by photoseparation of O^- was calculated with section of the process $\sigma = (6.5-7) \cdot 10^{-18}$ cm² [1]. The result of this calculation is represented in Fig. 4 by curve III. It can be seen that experimental results with $v_s > 9.5$ km/sec lie above it. With $v_s > 10$ km/sec the divergence between calculated and experimental results exceeds the error of the latter. Point 2, i.e., averaged values of j_λ , were obtained in [4]. Experiments were carried out in a shock tube with an internal channel diameter of 152 mm with $p_0 = 13$ Pa. Comparison of the data for these measurements with j_λ calculated according

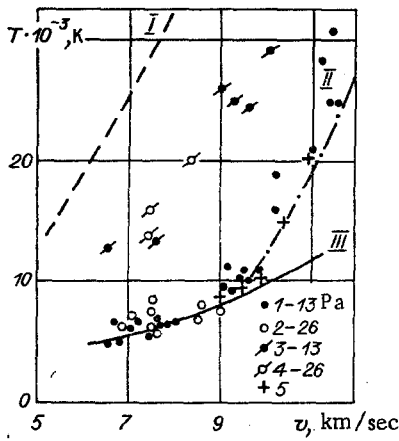


Fig. 3

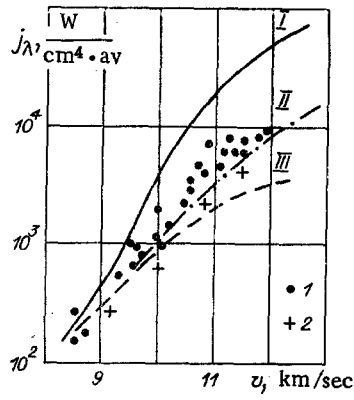


Fig. 4

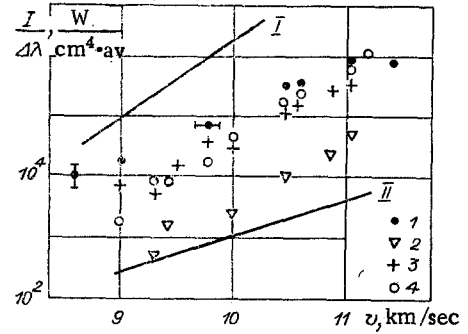


Fig. 5

to [1] shows that with $v_s \geq 10$ km/sec there is also the divergence noted above between calculation and experiment.

Shown in Fig. 5 are the results of measuring the emission of four oxygen lines in the infrared region of the spectrum $\lambda = 777.3; 794.9; 844.6; 926.3$ nm with $p_0 = 26$ Pa. Spectral characteristics of these lines are given in [1, 2]. In Fig. 5 the intensity of emission in these lines is determined in terms of emission I recorded by a spectrometer in the range $\Delta\lambda = 1.3$ nm containing the test line and the continuous spectrum background. The results of experiments presented make it possible to compare graphically the intensity of the spectral line and the background in an experiment. Curve II relates to the emission intensity for the continuous spectrum with $\lambda = 800$ nm in the spectral range in question, and I relates to the calculation of the equilibrium value for emission characteristics of the line $\lambda = 777.3$ nm. It can be seen that calculated values markedly exceed experimental values with $v_s > 8.5$ km/sec.

The mean square relative deviation of values of n_e measured by the probe method from the corresponding equilibrium values with $p_0 = 26$ Pa and $v_s = 4-9$ km/sec does not exceed 30%. With $v_s > 9$ km/sec the scatter of probe measurement results does not exceed $\pm 50\%$, and they are (see [6]) in good agreement with n_e measured from the Stark line broadening $H\beta$. The accuracy of this last method is estimated at $\sim 20\%$. Fewer measurements of n_e were carried out with $p_0 = 13.66$ Pa, and their analysis showed that n_e is determined with an accuracy to coefficient 2.

Values of T_e measured by the triple probe with $v_s \leq 9$ km/sec agree with the corresponding equilibrium values of mean square deviation of 7-10%. With $v_s > 9$ km/sec the accuracy of determining T_e is estimated at 20%.

The total error in determining emission intensity in the continuous spectrum and in lines is estimated at 60-70%. The error caused by the contribution of distant wings of lines not falling in the spectrum recording range, constitutes a small part of it since even for very broad lines ($\lambda = 794.9$ nm [2]) an estimate of the error due to nonconsideration of the wing lines (according to [13]) gives $\sim 12\%$. For all of the rest of the lines this error decreases by an order of magnitude or more.

3. As already noted, the difference in n_e behind a strong SW with low values of p_0 for calculated equilibrium values in [5] is explained by absence in the gas sample of local thermodynamic equilibrium due to the effect of lighting up in the population density of excited levels for N and O atoms. Under the conditions in question absence of LTE is confirmed by nonfulfillment of the Grim criterion [13] for optical transmittance of the plasma:

$$n_e \geq 10^{18} \left(\frac{E_r}{E_i} \right)^3 \left(\frac{kT_e}{E_i} \right)^{1/2}, \text{ cm}^{-3}, \quad (3.1)$$

where E_i is atom ionization energy; E_r is excitation energy of the resonance level. Under experimental conditions (3.1) is reduced to a requirement of $n_e \geq 10^{17}$ cm $^{-3}$. Measured values are $n_e < 2 \cdot 10^{16}$ cm $^{-3}$ ($p_0 = 26$ Pa, $v_s \leq 15$ km/sec), and with $v_s = 10-11$ km/sec, $n_e = (2-4) \cdot 10^{15}$ cm $^{-3}$. Another process which may affect n_e in a sample of relatively small dimensions is diffusion.

A criterion governing the condition with which an effect on n_e of diffusion processes might be expected may be obtained by making the well-known analogy between gas flow in a sample behind an incident SW and in the shock layer around a critical point of a blunt body. A correlation relationship $n_e/n_{ep} = K$ is given in [14] for a viscous shock layer in a region of the critical point for a body with a blunting radius R [$K = Re_0 \Lambda_i^2 / (1 + \Lambda_i^2)$], Re_0 is Reynolds number for conditions in the retardation region ($Re_0 = u_\infty \rho_\infty R / \mu_0$), μ_0 is viscosity, $\Lambda_i = \tau / \tau_i$, τ is typical gas-dynamic flow time, τ_i is ionization time behind a direct SW]. The ratio $n_e/n_{ep} < 1$ if $K < 10^3$. In the case of the conditions in question behind the SW in the sample it is possible to introduce $Re_s = v_s \rho_1 \Delta / \mu_1$ (ρ_1 and μ_1 are density and viscosity behind the SW, Δ is sample thickness) and the corresponding correlation parameter K_s . Calculation shows that with $v_s = 10$ - 11 km/sec, $p_0 = 26$ Pa, $\Delta \approx 3$ cm, $K_s \approx 10^3$. Thus, under the conditions being considered apparently diffusion does not markedly affect the electron concentration in the sample. A marked effect of diffusion should be expected with $p_0 < 6.5$ Pa.

With $v_s \geq 10$ km/sec the degree of gas ionization behind the SW $\alpha_i \geq 0.1$ and E_i becomes a marked term of total internal energy (with $v_s = 11$ km/sec, $E_i = 0.2E$). In this case absence of equilibrium for ionization affects the main thermodynamic parameters of the gas behind the SW. In particular, a reduction in the level of ionization should lead to an increase in gas temperature T for the sample. Results of calculating T taking account of the measured values of n_e and data for thermodynamic calculation of the state of a gas behind the SW in the presence of LTE [12] are represented in Fig. 3 by curve II. It can be seen that the calculated curve is in good agreement with the results of measuring T_e . It is noted that the time for establishing equilibrium from the temperature between ions and electrons under experimental conditions [13] $\tau_{i,e} = 3 \cdot 10^{-7}$ sec $\ll \tau$.

Taking account of the increase in T in the sample behind the SW the dependence on v_s of emission coefficient j_λ was recalculated in the region of the continuous spectrum with $\lambda = 510$ nm. Corresponding curve II in Fig. 4 is the best conformity with experimental results.

From data presented in Fig. 5 it can be seen that the population densities for excited atomic levels in a quasisteady gas sample differ from equilibrium. Under regimes of the simplest approach [5] the population density for the level of j in an optically incomplete plasma may be presented in the form

$$n_j = n_{jp} / (1 + \tau_c / \tau_r), \quad (3.2)$$

where n_{jp} is equilibrium population density level; τ_r is rational life time; τ_c is characteristic time for emissionless collision transfer (extinction time in collisions). It is assumed that for levels relating to the test lines of the oxygen spectrum values of τ_c / τ_r are identical. The distribution of population densities may be characterized by excitation temperature T_B . Results of determining it by the relative intensity method are represented in Fig. 3 by points 5. It is typical that T_B agrees with T_e and T .

LITERATURE CITED

1. V. A. Kamenshchikov, Yu. A. Plastinin, V. M. Nikolaev, and L. A. Novitskii, Radiation Properties of Gases at High Temperatures [in Russian], Mashinostroenie, Moscow (1971).
2. I. V. Avilova, L. M. Biberman, V. S. Vorob'ev, et al., Optical Properties of Hot Air [in Russian], Nauka, Moscow (1970).
3. R. A. Allen, A. Textoris, and J. Wilson, "Measurements of free-bound and free-free continua of nitrogen, oxygen and air," J. Quant. Spectrosc. Radiat. Transfer, 5, 95 (1965).
4. J. Wilson, "Ionization rate of air behind high-speed shock waves," Phys. Fluids, 9, No. 10 (1965).
5. G. N. Zalogin, V. V. Lunev, and Yu. A. Plastinin, "Ionization and nonequilibrium emission of air behind strong shock waves," Izv. Akad. Nauk SSSR, Mekh. Zhidk. Gaza, No. 1, (1980).
6. V. A. Gorelov and L. A. Kil'dyushova, "Results of probe measurements for ionization of air behind strong shock waves," Pis'ma Zh. Tekh. Fiz., 7, No. 21 (1981).
7. W. E. Sharfman and W. C. Taylor, "Use of ion probes in supersonic plasma flow," AIAA J., 8, No. 6 (1970).
8. M. K. Gladyshev, V. K. Gorelov, and V. M. Chernyshev, "Electrical discharge shock tube for aerophysical studies," Probl. Fiz. Gaz. Dinam. (Tr. TsAGI), No. 1656 (1975).
9. J. De Vos, "A new determination of the emissivity of tungsten ribbon," Physica, 20, No. 10 (1954).

10. V. A. Gorelov and L. A. Kil'dyushova, "Features of electrical probe characteristics in a transfer regime in a supersonic plasma flow," *Teplofiz. Vys. Temp.*, **23**, No. 2 (1985).
11. Chen Sin-Li and T. Sekiguchi, "Instantaneous direct-display system of plasma parameters by means of a triple probe," *J. Appl. Phys.*, **36**, No. 10 (1965).
12. N. M. Kuznetsov, *Thermodynamic Functions and Shock Adiabats for Air at High Temperatures* [in Russian], Mashinostroenie, Moscow (1965).
13. G. Grim, *Plasma Spectroscopy* [in Russian], Atomizdat, Moscow (1969).
14. V. A. Gorelov, A. S. Korolev, and V. S. Nikol'skii, "Ionization of a gas in a viscous shock layer and modeling of this process in a laboratory experiment," *Zh. Prikl. Mekh. Tekh. Fiz.*, No. 6 (1985).

DIFFUSION MODEL OF VIBRATIONAL RELAXATION IN A BINARY MIXTURE OF
DIATOMIC MOLECULES (QUANTUM OSCILLATORS)

O. V. Skrebkov

UDC 533.601.18

Chemical activation of a system involving the crossing of an activation barrier was treated for the first time by Kramers [1] as a stochastic diffusion process in phase space with the use of the formalism of the theory of Brownian motion due to Einstein. In later years the diffusion model was applied to various kinetic processes such as condensation [2], electronic excitation and ionization [2], the approach to equilibrium of the translational degrees of freedom of molecules (TT-relaxation) [3], rotational-translational RTT and RT-relaxation [4, 5], vibrational-translational VT-relaxation [6-9] (including dissociation and recombination [10-12] and radiative deactivation [13]), vibrational-rotational-translational VRT-relaxation and dissociation [14], vibrational VVT-relaxation in a one-component gas [15-17] (including loss of excited particles in chemical reactions [18]), and vibrational VVV'T-relaxation in binary gas mixtures [19-22].

In all of these cases the term "diffusion process" refers to one-dimensional [1-3, 5-18, 20-23] or two-dimensional [4, 14, 19] diffusion in the continuous space of the momenta, angular momenta, and (or) the energies (or the corresponding quantum numbers*) and is described by a generalized diffusion equation of the Fokker-Planck type or by a system of such equations when there are discrete states [22, 23]. The fundamental condition for the applicability of the diffusion model is that the change $\Delta\varepsilon$ of a coordinate ε (such as the vibrational or rotational energy, angular momentum, mass of a condensation nucleus) must be small in an elementary event, such as a vibrational or rotational transition, the attachment of a molecule to a condensation nucleus, and so on. That is

$$\Delta\varepsilon \ll \varepsilon \text{ or } n \ll \nu \quad (1.1)$$

(ν is the quantum number and n is its change in an elementary event). On the other hand, in relaxation problems the space of the problem (energy or the corresponding quantum number, for example) can be approximated as continuous only if the system is classical. For example, if ε is the energy of an oscillator, then $\varepsilon \approx kT$ and the classical diffusion model will be applicable if

$$\Delta\varepsilon \ll kT \text{ or } n\hbar\omega_0 \ll kT, \quad (1.2)$$

where $\Delta\varepsilon$ is the change in the vibrational energy due to a collision; n is the change in the vibrational quantum number; $\omega_\nu \equiv \omega_{\nu+1, \nu}$ is the frequency of the vibrational transition $\nu + 1 \rightarrow \nu$; T is the temperature; k is the Boltzmann constant.

It is not difficult to see that when there are transitions between highly-excited states, the condition (1.1) is significantly less strict than (1.2). When we have transitions between low-lying states and multiquantum transitions can be neglected ($n = 1$), the single-quantum system of balance equations for the population densities can be written without

*In the treatment of condensation according to the theory of Zel'dovich (1942; see [2]), the process is diffusion in the "space" of the sizes of the nuclei of the condensed phase.